*Proc. Camb. Phil. Soc.* (1967), **63**, 513
*With 6 text-figures*
PCPS 63–63
*Printed in Great Britain*



# Fluctuating boundary layer on a magnetized plate

BY SAHIB SINGH CHAWLA
*Indian Institute of Technology, Kharagpur*

(*Received* 30 *July* 1966)

The laminar boundary layer on a magnetized plate, when the magnetic field oscillates in magnitude about a constant non-zero mean, is analysed. For low-frequency fluctuations the solution is obtained by a series expansion in terms of a frequency parameter, while for high frequencies the flow pattern is of the 'skin-wave' type unaffected by the mean flow. In the low-frequency range, the phase lead and the amplitude of the skin-friction oscillations increase at first and then decrease to their respective 'skin-wave' values. On the other hand the phase angle of the surface current decreases from 90° to 45° and its amplitude increases with frequency.

1. *Introduction.* This paper is devoted to a study of magnetohydrodynamic boundary layer in uniform flow past a semi-infinite plate, when a magnetic field, fluctuating about a non-zero mean in the stream direction, is applied at the plate. The basic steady flow in the case of a uniform field has been investigated by Glauert (1). The specific aim of the present study is to gain further insight into the flow of a conducting fluid of small viscosity when the field is not uniform. The possibility of setting up a uniform field in the plate, physically, has been very well discussed by Zhigulev (3) and Glauert (1). In order to create a fluctuating magnetic field, we join the plate (in the manner of Zhigulev) or the solenoid (in the manner of Glauert) with d.c. and a.c. generators placed in series. It is assumed, of course, that the amplitude of the superimposed oscillating magnetic field is much smaller than the uniform component.

We have reconsidered the basic steady flow using Karman–Pohlhausen technique, and obtained an approximate solution to be used in the subsequent study of unsteady flow. Two different solutions for low- and high-frequency ranges are obtained. The method of solving the problem is essentially the same as developed by Lighthill (2). Here, of course, we have extended Lighthill's treatment to obtain a series solution for low frequencies. It is found that there are wave-like-disturbances (which are in fact hydromagnetic waves) within the boundary layer. At the highest frequencies these waves degenerate into skin waves. As remarked by Lighthill (2), the Karman–Pohlhausen method leads to fairly accurate physical properties although details may be in error.

2. *The basic equations.* We consider the two-dimensional flow of an incompressible, viscous, electrically conducting fluid past a semi-infinite flat plate, when both the Reynolds' number and the magnetic Reynolds' number are large. There is no magnetic field in the distant fluid, but in the boundary layer there is a field in the stream direction



https://doi.org/10.1017/S0305004100041463 Published online by Cambridge University Press

generated by external means within the plate itself. If $(u, v)$ and $(H_x, H_y)$ are the velocity and magnetic field components respectively. the equations which govern the flow in the boundary layer, in MKS units, are:

$$\frac{\partial u}{\partial t}+u\frac{\partial u}{\partial x}+v\frac{\partial u}{\partial y}=\nu\frac{\partial^2 u}{\partial y^2}+\frac{\mu}{\rho}\left[H_x\frac{\partial H_x}{\partial x}+H_y\frac{\partial H_x}{\partial y}\right], \tag{1a}$$

$$\frac{\partial H_x}{\partial t}+u\frac{\partial H_x}{\partial x}+v\frac{\partial H_x}{\partial y}-H_x\frac{\partial u}{\partial x}-H_y\frac{\partial u}{\partial y}=\eta\frac{\partial^2 H_x}{\partial y^2}, \tag{1b}$$

$$\frac{\partial u}{\partial x}+\frac{\partial v}{\partial y}=0, \tag{1c}$$

$$\frac{\partial H_x}{\partial x}+\frac{\partial H_y}{\partial y}=0. \tag{1d}$$

The fluid has density $\rho$, kinematic viscosity $\nu$, electrical conductivity $\sigma$ and magnetic permeability $\mu$. Also $\eta$, the magnetic diffusivity, is defined as

$$\eta=(\mu\sigma)^{-1}. \tag{2}$$

The boundary conditions, to be satisfied, are

$$\left.\begin{aligned} y=0: &\quad u=0, \quad v=0, \quad H_x=H_0(1+\epsilon\cos\omega t),\\ \to\infty: &\quad u\to U_0, \quad H_x=0, \quad H_y=0, \end{aligned}\right\} \tag{3}$$

where $\omega$ is the frequency of the field fluctuations and $\epsilon \ll 1$.

We write $u, v, H_x$ and $H_y$ as the sum of the steady and small oscillating components as

$$\left.\begin{aligned} u&=u_s+\epsilon u_1 e^{i\omega t}, \quad H_x=H_{xs}+\epsilon H_{x1}e^{i\omega t},\\ v&=v_s+\epsilon v_1 e^{i\omega t}, \quad H_y=H_{ys}+\epsilon H_{y1}e^{i\omega t}, \end{aligned}\right\} \tag{4}$$

where $u_s$, $v_s$, $H_{ys}$, $H_{xs}$ is the steady mean flow and satisfies the equations:

$$u_s\frac{\partial u_s}{\partial x}+v_s\frac{\partial u_s}{\partial y}=\nu\frac{\partial^2 u_s}{\partial y^2}+\frac{\mu}{\rho}\left[H_{xs}\frac{\partial H_{xs}}{\partial x}+H_{ys}\frac{\partial H_{xs}}{\partial y}\right], \tag{5a}$$

$$u_s\frac{\partial H_{xs}}{\partial x}+v_s\frac{\partial H_{xs}}{\partial y}-H_{xs}\frac{\partial u_s}{\partial x}-H_{ys}\frac{\partial u_s}{\partial y}=\eta\frac{\partial^2 H_{xs}}{\partial y^2}, \tag{5b}$$

$$\frac{\partial u_s}{\partial x}+\frac{\partial v_s}{\partial y}=0, \tag{5c}$$

$$\frac{\partial H_{xs}}{\partial x}+\frac{\partial H_{ys}}{\partial y}=0, \tag{5d}$$

with the boundary conditions:

$$\left.\begin{aligned} y=0: &\quad u_s=0, \quad v_s=0, \quad H_{xs}=H_0,\\ y\to\infty: &\quad u_s\to U_0, \quad H_x=0, \quad H_y=0. \end{aligned}\right\} \tag{6}$$

https://doi.org/10.1017/S0305004100041463 Published online by Cambridge University Press

Neglecting squares of $\epsilon$ and dividing by $e^{i\omega t}$, we find that $u_1, v_1, H_{x1}, H_{y1}$ satisfy the following differential equations

$$i\omega u_1 + u_1 \frac{\partial u_s}{\partial x} + u_s \frac{\partial u_1}{\partial x} + v_1 \frac{\partial u_s}{\partial y} + v_s \frac{\partial u_1}{\partial y}$$
$$= \nu \frac{\partial^2 u_1}{\partial y^2} + \frac{\mu}{\rho}\left[H_{x1}\frac{\partial H_{xs}}{\partial x} + H_{xs}\frac{\partial H_{x1}}{\partial x} + H_{y1}\frac{\partial H_{xs}}{\partial y} + H_{ys}\frac{\partial H_{x1}}{\partial y}\right], \tag{7a}$$

$$i\omega H_{x1} + u_1 \frac{\partial H_{xs}}{\partial x} + u_s \frac{\partial H_{x1}}{\partial x} + v_1 \frac{\partial H_{xs}}{\partial y} + v_s \frac{\partial H_{x1}}{\partial y}$$
$$- H_{x1}\frac{\partial u_s}{\partial x} - H_{xs}\frac{\partial u_1}{\partial x} - H_{y1}\frac{\partial u_s}{\partial y} - H_{ys}\frac{\partial u_1}{\partial y} = \eta \frac{\partial^2 H_{x1}}{\partial y^2}, \tag{7b}$$

$$\frac{\partial u_1}{\partial x} + \frac{\partial v_1}{\partial y} = 0, \tag{7c}$$

$$\frac{\partial H_{x1}}{\partial x} + \frac{\partial H_{y1}}{\partial y} = 0, \tag{7d}$$

with the boundary conditions:

$$\left.\begin{aligned} y = 0: &\quad u_1 = 0, \quad v_1 = 0, \quad H_{x1} = H_0, \\ y \to \infty: &\quad u_1 \to 0, \quad H_{x1} = 0, \quad H_{y1} = 0. \end{aligned}\right\} \tag{8}$$

3. *Steady-state solution.* Equations (5)–(6) are the magnetohydrodynamic boundary-layer equations which describe the steady flow of an electrically conducting fluid past a semi-infinite magnetized plate. Glauert (2) has solved these equations, using of course the integrated form of (5*b*), for large and small conductivities (and strong and weak applied magnetic fields). Briefly, the method employed by Glauert consists of matching systematically solutions valid in the 'inner' and 'outer' layers. It is evident that to solve (7)–(8), the basic steady flow must be known. We have, therefore, re-considered equations (5)–(6) and solved them by Karman–Pohlhausen method.

Integrating (5*a*) and (5*b*) over the width of the boundary layer and making use of (5*c*) and (5*d*), we obtain

$$\nu\left(\frac{\partial u_s}{\partial y}\right)_{y=0} = U_0^2 \frac{d}{dx}\left[\int_0^\infty \frac{u_s}{U_0}\left(1 - \frac{u_s}{U_0}\right) dy - \beta \int_0^\infty \frac{H_{xs}}{H_0}\left(1 - \frac{H_{xs}}{H_0}\right) dy\right], \tag{9a}$$

$$\eta\left(\frac{\partial H_{xs}}{\partial y}\right)_{y=0} = 0, \tag{9b}$$

where
$$\beta = \mu H_0^2/\rho U_0^2. \tag{10}$$

Also at $y = 0$, (5*a*) and (5*b*) give

$$\nu\left(\frac{\partial^2 u_s}{\partial y^2}\right)_{y=0} = -\frac{\mu}{\rho} H_{ns}\left(\frac{\partial H_{xs}}{\partial y}\right)_{y=0}, \tag{11a}$$

$$\eta\left(\frac{\partial^2 H_{xs}}{\partial y^2}\right)_{y=0} = -H_{ns}\left(\frac{\partial u_s}{\partial y}\right)_{y=0}, \tag{11b}$$



https://doi.org/10.1017/S0305004100041463 Published online by Cambridge University Press

where $H_{ns}$ is the normal component of the magnetic intensity at the plate. Consistent with (6), (9$b$) and (11) we assume the steady-state velocity distribution $u_s$ and the magnetic field distribution $H_{xs}$ to be given by

$$\frac{u_s}{U_0} = \frac{2y}{\delta_1} - \frac{2y^3}{\delta_1^3} + \frac{y^4}{\delta_1^4}, \tag{12a}$$

$$\frac{H_{xs}}{H_0} = 1 - \frac{6y^2}{\delta_2^2} + \frac{8y^3}{\delta_2^3} - \frac{3y^4}{\delta_2^4}, \tag{12b}$$

where $\delta_1$ and $\delta_2$ are the thicknesses of the viscous and magnetic boundary layers, and satisfy

$$\delta_2 \frac{\partial \delta_2}{\partial x} = \frac{15\eta}{U_0} \frac{\delta_1}{\delta_2}. \tag{13}$$

Substitution of (12) in (9$a$) gives

$$\frac{2\nu}{U_0} = \delta_1 \frac{d}{dx}\left[\frac{37}{315}\left(1 - \frac{36}{37}\Delta\beta\right)\delta_1\right], \tag{14}$$

where

$$\Delta = \delta_2/\delta_1. \tag{15}$$

Considering only the case of similarity solutions, equations (13), (14) and (15) give

$$\delta_1 = 2\left[\frac{\nu x}{U_0} \frac{315}{37 - 36\Delta\beta}\right]^{\frac{1}{2}}, \tag{16a}$$

$$\delta_2 = 2\left[\frac{\eta x}{U_0} \frac{15}{2\Delta}\right]^{\frac{1}{2}}, \tag{16b}$$

and, therefore

$$42\Delta^3 = \lambda(37 - 36\Delta\beta), \tag{17}$$

where

$$\lambda = \eta/\nu. \tag{18}$$

(17) is a cubic in $\Delta$, having only one positive real root. For given values of $\lambda$ and $\beta$, $\Delta$ can be easily calculated and hence all other quantities of physical interest can be obtained. For weak applied magnetic fields, we find from (17) that $\Delta < 1$ when the electrical conductivity of the fluid is large and $\Delta > 1$ for small conductivity. $\Delta$ decreases as the strength of the applied magnetic field is increased and ultimately $\Delta < 1$ (for all conductivities) for sufficiently strong fields. Due to the finite conductivity of the fluid, the induced current within the boundary layer tends to spread away from the wall, pushing the vorticity out of the magnetic boundary layer. This results in the thickening of the boundary layers. Moreover, the fluid near the plate experiences a resistance in forcing its way past the field lines which emerge from the plate to supply the magnetic flux in the boundary layer. Hence the skin friction at the plate can be expected to decrease with increasing magnetic field.

The skin friction $T$, at the plate, is given by

$$T/T_0 = (42\Delta^3/37\lambda)^{\frac{1}{2}}, \tag{19}$$

where $T_0$ is the corresponding value of $T$ in the non-magnetic case. Also the normal component of the magnetic intensity at the plate is given by

$$H_{ns}/H_0 = (6\eta/5x\Delta U_0)^{\frac{1}{2}}. \tag{20}$$

https://doi.org/10.1017/S0305004100041463 Published online by Cambridge University Press

The total drag (shear stress) per unit area is, therefore,

$$T_D = T + \mu H_0 H_{ns} = T(1 + 3\lambda\beta/\Delta^2). \tag{21}$$

The skin friction $T$ and total drag $T_D$ at the plate are tabulated against $\beta$ for $\lambda = 0{\cdot}1, 1, 10$ in Table 1. We find that the skin friction decreases as $\beta$ increases but the total drag increases.

Table 1

| | $\lambda = 0{\cdot}1$ | | $\lambda = 1$ | | $\lambda = 10$ | |
|---|---|---|---|---|---|---|
| $\beta$ | $T/T_0$ | $T_D/T_0$ | $T/T_0$ | $T_D/T_0$ | $T/T_0$ | $T_D/T_0$ |
| 0·05 | 0·9891 | 1·0651 | 0·9768 | 1·1413 | 0·9502 | 1·3079 |
| 0·1 | 0·9784 | 1·0311 | 0·9539 | 1·2855 | 0·9014 | 1·6295 |
| 0·25 | 0·9463 | 1·3321 | 0·8859 | 1·7356 | 0·7613 | 2·6869 |
| 0·5 | 0·8939 | 1·6804 | 0·7419 | 2·4339 | 0·5619 | 4·8233 |
| 0·75 | 0·8428 | 2·0459 | 0·6709 | 3·4270 | 0·4101 | 7·5096 |
| 1 | 0·7931 | 2·4301 | 0·5878 | 4·4849 | 0·3036 | 10·7675 |

To obtain his series solution in case of weak applied magnetic fields ($\beta$ small) Glauert (1) assumes that $\beta\lambda^{\frac{1}{2}}$ is small for large conductivities ($\lambda$ small) and $\beta \log \lambda$ is small for small conductivities ($\lambda$ large). Under these limitations our results are in reasonably good agreement with Glauert's series solution. Glauert has also shown that the boundary layer separates from the surface for sufficiently large values of the applied field strength. In particular, when $\lambda = 10$ separation occurs for $\beta = \beta_0 = \pi (\log \lambda)^{-1} = 1{\cdot}37$. But the thickness of the boundary layer grows significantly with the strength of the applied field, and as such the averaging process, adopted here, may not lead to very accurate results. In view of this the following analysis will be restricted only to moderate strength of the applied mean magnetic field. Nevertheless, the Karman–Pohlhausen method proves itself to be a successful tool in predicting the trend as to how the flow is likely to be affected with the increase of the field strength.

4. *Superimposed unsteady solution.* We have already obtained the basic steady flow using Karman–Pohlhausen method. We shall employ the same method to solve (7)–(8). Integrating (7$a$) and (7$b$) over the boundary-layer thickness, we obtain the averaging conditions as

$$\nu \left(\frac{\partial u_1}{\partial y}\right)_{y=0} + \frac{\mu H_0 H_{ns}}{\rho} = -i\omega U_0 \int_0^\infty \frac{u_1}{U_0}\, dy + U_0^2 \frac{d}{dx} \int_0^\infty \left[\beta \left(\frac{2H_{x1}}{H_0}\frac{H_{xs}}{H_0} - \frac{H_{x1}}{H_0}\right) - \left(\frac{2u_1}{U_0}\frac{u_s}{U_0} - \frac{u_1}{U_0}\right)\right] dy, \tag{22a}$$

$$\eta \left(\frac{\partial H_{x1}}{\partial y}\right)_{y=0} = -i\omega H_0 \int_0^\infty \frac{H_{x1}}{H_0}\, dy. \tag{22b}$$

Also at $y = 0$, (7$a$) and (7$b$) give

$$\nu \left(\frac{\partial^2 u_1}{\partial y^2}\right)_{y=0} = -\frac{\mu H_{ns}}{\rho} \left(\frac{\partial H_{x1}}{\partial y}\right)_{y=0}, \tag{23a}$$

$$i\omega H_0 - \left(H_{y1}\frac{\partial u_s}{\partial y}\right)_{y=0} - H_{ns}\left(\frac{\partial u_1}{\partial y}\right)_{y=0} = \eta \left(\frac{\partial^2 H_{x1}}{\partial y^2}\right)_{y=0}. \tag{23b}$$

https://doi.org/10.1017/S0305004100041463 Published online by Cambridge University Press

Consistent with the boundary conditions, we assume the following expressions for $u_1$ and $H_{x1}$:

$$\frac{u_1}{U_0} = A_1\left(\frac{y}{\delta_1} - \frac{3y^3}{\delta_1^3} + \frac{2y^4}{\delta_1^4}\right) - \frac{3\lambda\beta}{\Delta^3} B_1\left(\frac{y^2}{\delta_1^2} - \frac{2y^3}{\delta_1^3} + \frac{y^4}{\delta_1^4}\right), \tag{24a}$$

$$\frac{H_{x1}}{H_0} = 1 - \frac{4y^3}{\delta_2^3} + \frac{3y^4}{\delta_2^4} + B_1\left(\frac{y}{\delta_2} - \frac{3y^3}{\delta_2^3} + \frac{2y^4}{\delta_2^4}\right) + B_2\left(\frac{y^2}{\delta_2^2} - \frac{2y^3}{\delta_2^3} + \frac{y^4}{\delta_2^4}\right). \tag{24b}$$

Substituting these expressions for $u_1$ and $H_{x1}$ in (22) and (23) we find that $A_1$, $B_1$ and $B_2$ are given by

$$B_1 = -(i\omega^*)\frac{3\Delta^2}{5\lambda}\left(1 + \frac{B_1}{4} + \frac{B_2}{18}\right), \tag{25a}$$

$$3A_1 + B_2 + \tfrac{1}{2}\left(1 + 2x\frac{d}{dx}\right)\left(B_2 + \frac{9B_1}{2}\right) = \frac{i\omega^*\Delta^2}{\lambda} - 9, \tag{25b}$$

$$A_1 + \frac{\lambda}{7\Delta^3}\left(1 + 2x\frac{d}{dx}\right)\left[\frac{37A_1}{6} + \beta\Delta\left(B_2 + \frac{4\Delta^4 - 11\lambda}{2\Delta^4}B_1\right)\right] = \frac{i\omega^*}{20}\left(\frac{2\lambda\beta}{\Delta^3}B_1 - 3A_1\right) - \frac{36\lambda\beta}{7\Delta^2}. \tag{25c}$$

In the above equations $\omega^*$ is the non-dimensional frequency parameter defined as

$$\omega^* = \omega\delta_1^2/\nu. \tag{26}$$

Equations (25) may be solved by expanding $A_1$, $B_1$, and $B_2$ in series of the form

$$A_1 = \sum_{n=0}^{\infty} A_{1n}(i\omega^*)^n, \tag{27a}$$

$$B_1 = \sum_{n=0}^{\infty} B_{1n}(i\omega^*)^n, \tag{27b}$$

$$B_2 = \sum_{n=0}^{\infty} B_{2n}(i\omega^*)^n. \tag{27c}$$

Substituting (27) in (25) and comparing the coefficients of like powers of $\omega^*$ on both sides, we get

$$A_{10} = \frac{-12\lambda\beta}{2\lambda\beta + 7\Delta^2}, \quad B_{10} = 0, \quad B_{20} = \frac{6(2\lambda\beta - 7\Delta^2)}{2\lambda\beta + 7\Delta^2}, \tag{28a}$$

$$\left.\begin{aligned} A_{11} &= \frac{21\lambda\beta\Delta^2}{(36\lambda\beta + 70\Delta^2)(2\lambda\beta + 7\Delta^2)}\left[\frac{3}{2} - \frac{37 - 17\beta\Delta}{35\Delta} - \frac{11(4\lambda\beta + 7\Delta^2)}{14\Delta^4}\right], \\ B_{11} &= \frac{-2\Delta^2(4\lambda\beta + 7\Delta^2)}{5\lambda(2\lambda\beta + 7\Delta^2)}, \\ B_{21} &= \frac{7\lambda\Delta^2}{5(36\lambda\beta + 70\Delta^2)(2\lambda\beta + 7\Delta^2)}\left[-27\beta + \frac{2(148 - 63\beta\Delta)(74 - 21\beta\Delta)}{63\Delta^2} + \frac{99\beta(4\lambda\beta + 7\Delta^2)}{7\Delta^4}\right], \end{aligned}\right\} \tag{28b}$$

https://doi.org/10.1017/S0305004100041463 Published online by Cambridge University Press

and for $n \geqslant 2$, $A_{1n}$, $B_{1n}$, $B_{2n}$ are given by

$$B_{1n} = -\frac{3\Delta^2}{10\lambda}\left[\frac{B_{1n-1}}{2}+\frac{B_{2n-1}}{9}\right],$$

$$3A_{1n}+\tfrac{1}{2}(3+2n)B_{2n} = \frac{27\Delta^2(1+2n)}{40\lambda}\left[\frac{B_{1n-1}}{2}+\frac{B_{2n-1}}{9}\right],$$

$$\left[1+(1+2n)\frac{37\lambda}{42\Delta^3}\right]A_{1n}+(1+2n)\frac{\lambda\beta}{7\Delta^2}B_{1n}$$

$$= \frac{1}{20}\left(\frac{2\lambda\beta}{\Delta^3}B_{1n-1}-3A_{1n-1}\right)+\frac{3\beta(4\Delta^4-11\lambda)(1+2n)}{140\Delta^4}\left[\frac{B_{1n-1}}{2}+\frac{B_{2n-1}}{9}\right]. \quad (29)$$

The power series (27) are simultaneously absolutely convergent if the frequency parameter $\omega^* < \min(\rho_1, \rho_2, \rho_3)$ where

$$\overline{\lim_{n\to\infty}}\,|A_{1n}|^{1/n} = \frac{1}{\rho_1}; \quad \overline{\lim_{n\to\infty}}\,|B_{1n}|^{1/n} = \frac{1}{\rho_2}; \quad \overline{\lim_{n\to\infty}}\,|B_{2n}|^{1/n} = \frac{1}{\rho_3}.$$

The solution of equations (7) in the limiting case $\omega \to 0$ is the 'quasi-steady' solution to be denoted by $(u_0, v_0)$ and $(H_{x0}, H_{y0})$. These are the coefficients of $\epsilon$ in the velocity and magnetic field distributions for steady flow with an incident applied field $H_0(1+\epsilon)$. Hence

$$\left.\begin{aligned}(u_0, v_0) &= 2\beta(\partial/\partial\beta)(u_s, v_s),\\ (H_{x0}, H_{y0}) &= (H_{xs}, H_{ys})+2\beta(\partial/\partial\beta)(H_{xs}, H_{ys}).\end{aligned}\right\} \quad (29a)$$

That this solves equations (7) when $\omega = 0$ can be verified by direct substitution. It can also be verified easily that this quasi-steady solution corresponds to $A_{10}$, $B_{10}$, $B_{20}$ given by (28*a*). The quasi-steady solution may also be obtained directly from Glauert's results using (29*a*). The quasi-steady skin friction and magnetic drag as obtained by the present method agree qualitatively with the corresponding values as obtained from the available terms of Glauert's series solution.

(24*a*) and (24*b*) can now be expressed as the sum of the in-phase and out- of phase components as

$$\left.\begin{aligned}u_1 &= u_r + iu_2,\\ H_{x1} &= H_{xr} + iH_{x2}.\end{aligned}\right\} \quad (30)$$

The longitudinal components of the velocity and the magnetic fields may now be written in the form

$$\left.\begin{aligned}u &= u_s+\epsilon R_1\cos(\omega t+\phi_1),\\ H_x &= H_{xs}+\epsilon R_2\cos(\omega t+\phi_2),\end{aligned}\right\} \quad (31)$$

where

$$\left.\begin{aligned}R_1 &= (u_r^2+u_2^2)^{\frac{1}{2}}, \qquad \phi_1 = \tan^{-1}(u_2/u_r),\\ R_2 &= (H_{xr}^2+H_{x2}^2)^{\frac{1}{2}}, \quad \phi_2 = \tan^{-1}(H_{x2}/H_{xr}).\end{aligned}\right\}$$

Due to the fluctuations of the applied magnetic field, there are wave-like disturbances within the boundary layer. These disturbances are, in fact, hydromagnetic waves, which become more and more concentrated as the strength of mean applied field is increased. The wave-dominated flow pattern within the boundary layer is rather complicated, because there are several families of waves.

https://doi.org/10.1017/S0305004100041463 Published online by Cambridge University Press

At the highest frequencies, the hydromagnetic waves degenerate into skin (electromagnetic and shear) waves, confined to a very thin layer near the surface of the wall. Following the theory of differential equations with large coefficients, equation (7 *b*) may be simplified for large $\omega$ as

$$\eta \frac{\partial^2 H_{x1}}{\partial y^2} - i\omega H_{x1} = 0. \tag{32}$$

Its solution, subject to (8), is

$$H_{x1} = H_0 e^{-\sqrt{(i\omega/\eta)}\, y}, \tag{33}$$

which represents a 'skin-wave'. Physically, the skin effect dominates at the highest frequencies, and limits the penetration of the oscillating component of the field to a characteristic skin depth of order $(\eta/\omega)^{\frac{1}{2}}$.

At the wall,

$$H_{xs} = H_0, \quad H_{ys} = H_{ns}, \quad \frac{\partial H_{xs}}{\partial y} = 0 = \frac{\partial H_{ys}}{\partial y}.$$

Hence, following Lighthill (2), equation (7 *a*) can be approximated as

$$\nu \frac{\partial^2 u_1}{\partial y^2} - i\omega u_1 = \frac{\mu}{\rho} H_0 H_{ns} \sqrt{\frac{i\omega}{\eta}}\, e^{-\sqrt{(i\omega/\eta)}\, y} \tag{34}$$

near the wall. Solution of (34), subject to (8), is

$$u_1 = \frac{\mu H_0 H_{ns}}{\rho} \sqrt{\left(\frac{\eta}{i\omega}\right)} \frac{1}{\nu - \eta} \left(e^{-\sqrt{(i\omega/\eta)}\, y} - e^{-\sqrt{(i\omega/\nu)}\, y}\right) \tag{35}$$

showing that the velocity comprises of two wave modes.

The longitudinal components of the velocity and magnetic fields in the 'skin-wave' flow are

$$\left.\begin{aligned} u = u_s + \epsilon \frac{\mu H_0 H_{ns}}{\rho(\nu - \eta)} \left(\frac{\eta}{\omega}\right)^{\frac{1}{2}} \big[ & e^{-\sqrt{(\omega/2\eta)}\, y} \cos\left(\omega t - \tfrac{1}{4}\pi - \sqrt{(\omega/2\eta)}\, y\right) \\ & - e^{-\sqrt{(\omega/2\nu)}\, y} \cos\left(\omega t - \tfrac{1}{4}\pi - \sqrt{(\omega/2\nu)}\, y\right)\big], \\ H_x = H_{xs} + \epsilon H_0 e^{-\sqrt{(\omega/2\eta)}\, y} & \cos\left(\omega t - \sqrt{\omega/2\eta}\, y\right). \end{aligned}\right\} \tag{36}$$

We designate the two solutions (31) and (36) as low-frequency and 'skin-wave' solutions.

5. *Discussion of results.* The surface current in the 'skin-wave' flow is given by

$$J_\omega = -\left(\frac{\partial H_x}{\partial y}\right)_{y=0} = \epsilon H_0 \sqrt{\left(\frac{\omega}{\eta}\right)} \cos\left(\omega t + \tfrac{1}{4}\pi\right). \tag{37}$$

Its amplitude increases with frequency and its phase is ahead of the fluctuations of the applied magnetic field by 45°. On the other hand the skin friction in the 'skin-wave' flow is given by

$$T_\omega = \rho\nu \left(\frac{\partial u}{\partial y}\right)_{y=0} = T + \epsilon \frac{\mu H_0 H_{ns}}{1 + \lambda^{\frac{1}{2}}} \cos(\omega t + \pi), \tag{38}$$

https://doi.org/10.1017/S0305004100041463 Published online by Cambridge University Press

the amplitude of which is independent of frequency and its phase is 180° ahead of the applied field oscillations. Since the magnetic drag is $\mu H_0 H_n(1+\epsilon\cos wt)$, the total drag per unit area is

$$T_{\omega D} = T_D + \epsilon\frac{\mu H_0 H_{ns}\lambda^{\frac{1}{2}}}{1+\lambda^{\frac{1}{2}}}\cos\omega t, \tag{39}$$

which fluctuates in phase with the field. For low-frequency oscillations we have

$$\begin{aligned} J_\omega &= \epsilon\left[\frac{\partial H_{y1}}{\partial x} - \frac{\partial H_{x1}}{\partial y}\right]_{y=0} e^{i\omega t} \\ &= \epsilon H_0 \operatorname{Re}\left[-\frac{1}{\delta_2}\sum_{n=0}^{\infty} B_{1n}(i\omega^*)^n\right] e^{i\omega t}. \end{aligned} \tag{40a}$$

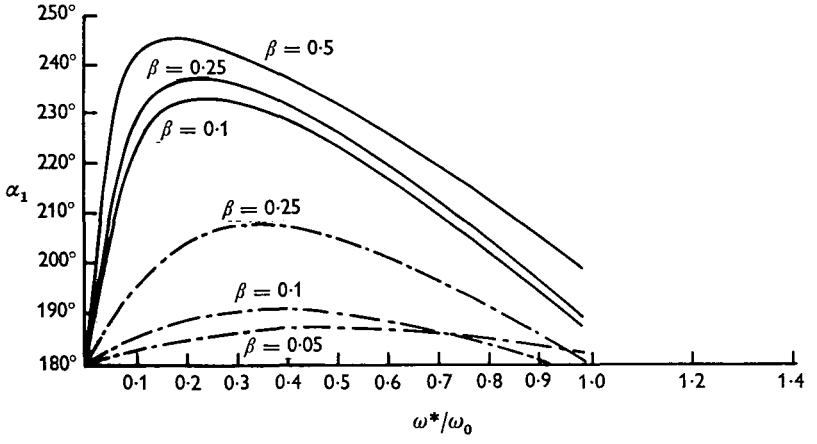



Fig. 1. Phase angle $\alpha_1$ of the oscillating skin friction.
$\lambda = 0{\cdot}1$ ———, $\lambda = 10$ —·—·—.

Here the term $\partial H_{y1}/\partial x$ has been neglected in comparison with $\partial H_{x1}/\partial y$ in view of the boundary-layer approximations used earlier. The skin-friction for low-frequency oscillations is given by

$$T_\omega = T + \epsilon\tfrac{1}{2}T\operatorname{Re}\left[\sum_{n=0}^{\infty} A_{1n}(i\omega^*)^n\right] e^{i\omega t} = T + \epsilon T_{\omega v}\cos(\omega t + \alpha_2) \quad \text{(say)}, \tag{40b}$$

and the magnetic drag $= \operatorname{Re}\mu H_0(1+\epsilon e^{i\omega t})(H_{ns}+\epsilon H_{n1}e^{i\omega t})$

$$\begin{aligned} &= \mu H_0 H_{ns} + \epsilon\mu H_0 \operatorname{Re}(H_{ns}+H_{n1})e^{i\omega t} \\ &= \mu H_0 H_{ns}\left[1+\epsilon\operatorname{Re}\left\{\frac{2(3\lambda\beta+7\Delta^2)}{2\lambda\beta+7\Delta^2}\right.\right. \\ &\qquad \left.\left. -\frac{5\lambda}{2\Delta^2}\sum_{n=1}^{\infty}(1+2n)B_{1n+1}(i\omega^*)^n\right\} e^{i\omega t}\right] \\ &= \mu H_0 H_{ns} + \epsilon T_{\omega H}\cos(\omega t+\alpha_3) \quad \text{(say)}. \end{aligned} \tag{40c}$$

The two solutions may be matched on the basis of surface-current oscillations, taking the matching point as the frequency at which the low-frequency solution predicts a phase advance equal to that of the 'skin-wave' solution. But we will com-

https://doi.org/10.1017/S0305004100041463 Published online by Cambridge University Press

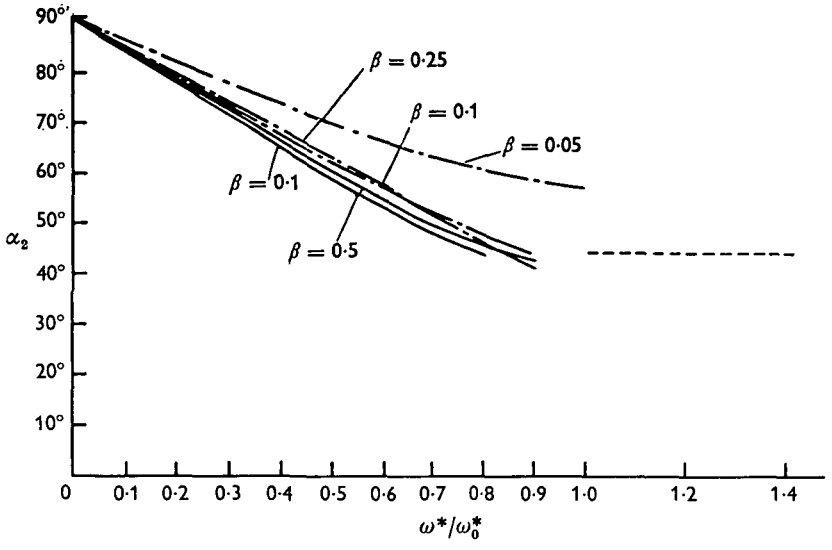



Fig. 2. Phase angle $\alpha_2$ of the surface current oscillations.
$\lambda = 0{\cdot}1$ ———, $\lambda = 10$ —·—·—.

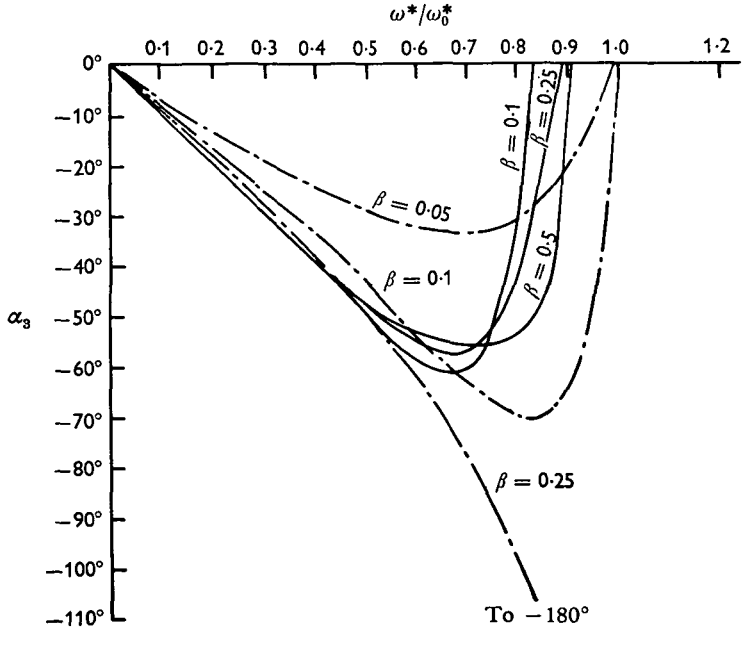



Fig. 3. Phase angle $\alpha_3$ of the oscillating magnetic drag.
$\lambda = 0{\cdot}1$ ———, $\lambda = 10$ —·—·—.

https://doi.org/10.1017/S0305004100041463 Published online by Cambridge University Press

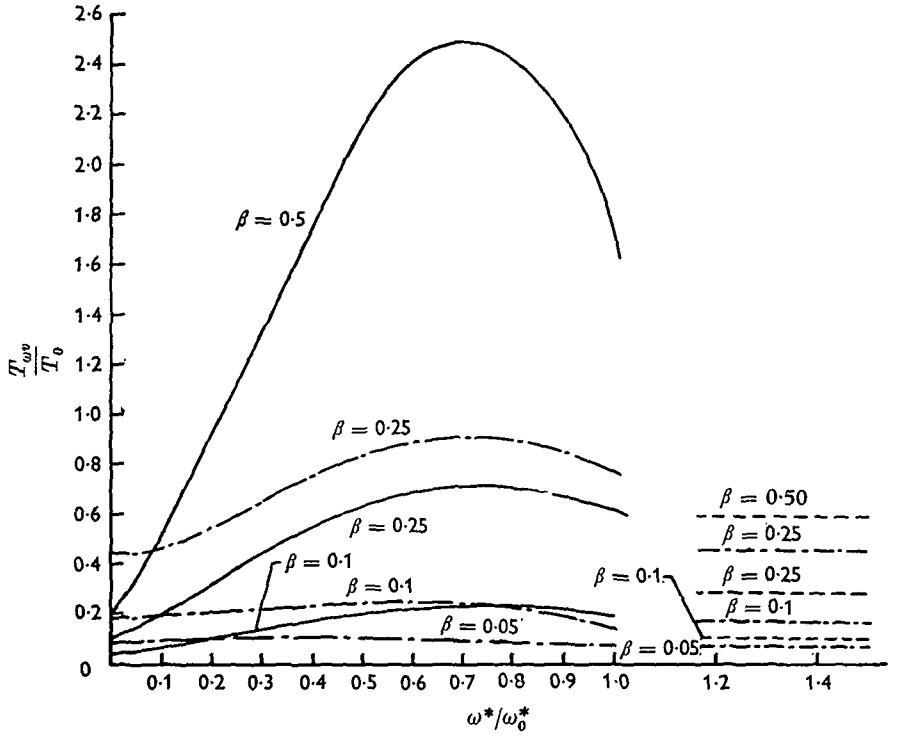



Fig. 4. Amplitude ($T_{\omega v}/T_0$) of the oscillating skin-friction.
Low-frequency: $\lambda = 0{\cdot}1$ ———, $\lambda = 10$ —·—.
Skin-wave: $\lambda = 0{\cdot}1$ – – – –, $\lambda = 10$ –·–·–.

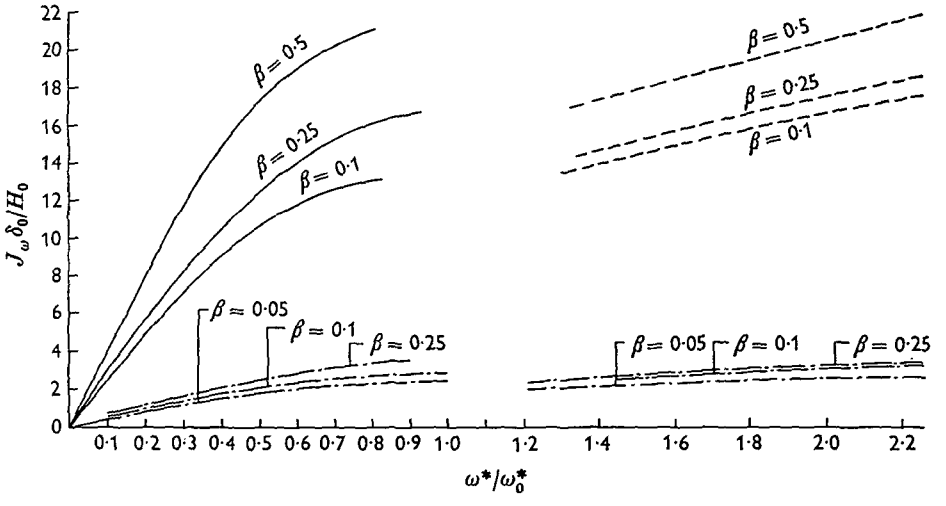



Fig. 5. Amplitude ($J_\omega \delta_0/H_0$) of the surface current oscillations.
$\delta_0$ is the non-magnetic boundary-layer thickness.
Low-frequency: $\lambda = 0{\cdot}1$ ———, $\lambda = 10$ —·—.
Skin-wave: $\lambda = 0{\cdot}1$ – – – –, $\lambda = 10$ –·–·–.

https://doi.org/10.1017/S0305004100041463 Published online by Cambridge University Press

pare the two solutions on the basis of total drag per unit area, to take into account the effect of convection by the moving fluid. Let $\alpha$ be the phase angle of the total drag corresponding to the low-frequency solution. We find the critical frequency parameter $\omega_0^*$ for which $\tan\alpha = 0$, giving $\alpha = n\pi$ $(n = 1, 2, \ldots,)$. It is found that $\omega_0^*$ increases as $\beta$ is

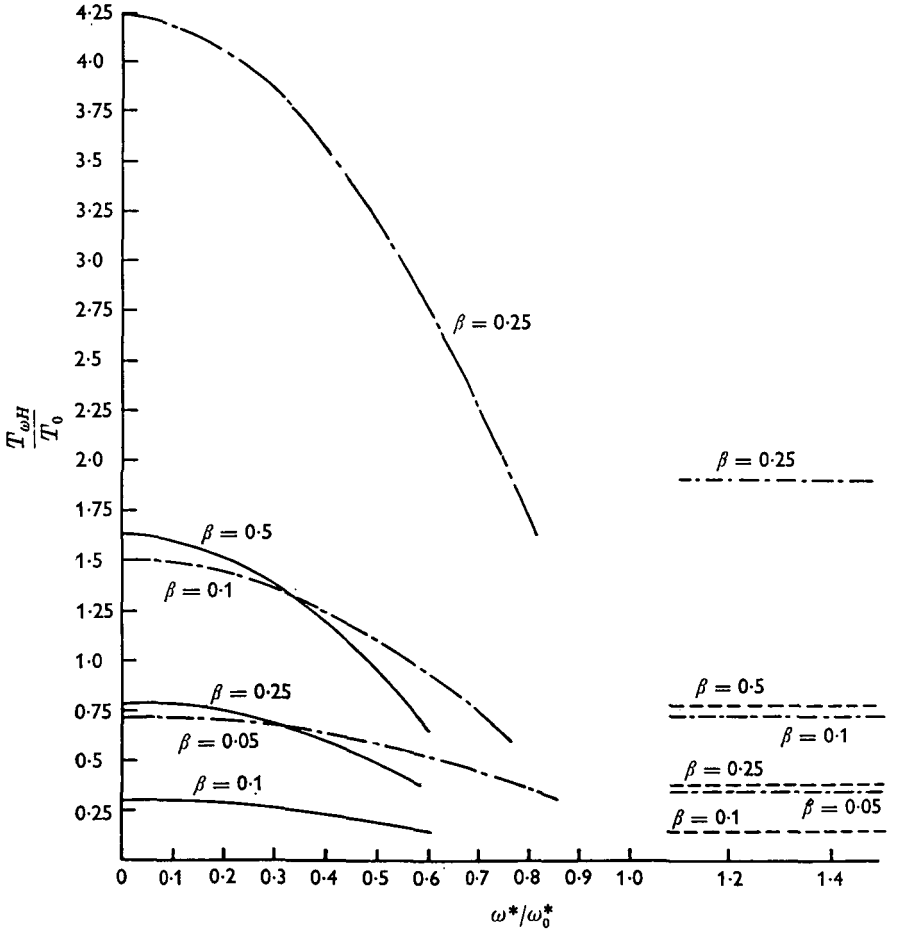



Fig. 6. Amplitude $(T_{\omega H}/T_0)$ of the oscillating magnetic drag.
Low-frequency: $\lambda = 0{\cdot}1$ ———, $\lambda = 10$ —·—.
Skin-wave: $\lambda = 0{\cdot}1$ – – – –, $\lambda = 10$ –·–·–.

increased, e.g. $\omega_0^* \approx 14{\cdot}4, 17{\cdot}3, 26{\cdot}5, 42{\cdot}8, 59{\cdot}8, 88{\cdot}9$, corresponding to $(\lambda = 0{\cdot}1, \beta = 0{\cdot}1)$; $(\lambda = 0{\cdot}1, \beta = 0{\cdot}25)$; $(\lambda = 0{\cdot}1, \beta = 0{\cdot}5)$; $(\lambda = 10, \beta = 0{\cdot}05)$; $(\lambda = 10, \beta = 0{\cdot}1)$; $(\lambda = 10, \beta = 0{\cdot}25)$ respectively. It shows that the hydromagnetic waves become more and more concentrated as the strength of the mean applied field is increased and accordingly the frequency, at which these waves degenerate into 'skin-waves' increases with $\beta$. The frequency response of the surface current, skin friction and magnetic drag as functions of $\omega^*/\omega_0^*$ are presented in Figures 1–6 for $\lambda = 0{\cdot}1$ and $\lambda = 10$ and various value of $\beta$.

In low-frequency solution, the results of the integral method indicate that the amplitude of the surface current increases with increasing frequency (this trend

https://doi.org/10.1017/S0305004100041463 Published online by Cambridge University Press

is the same for large frequency) but its phase angle decreases from 90° to 45° (corresponding to skin-wave solution) just before the frequency reaches its critical value $\omega_0^*$. The amplitude and the phase angle of the fluctuating components of the skin-friction increase for small frequencies. The amplitude and the phase lead after reaching peak values begin to decrease for higher frequencies and attain the asymptotic values just after the critical value $\omega_0^*$ is reached. On the other hand the amplitude of the magnetic drag decreases with frequency and attains its 'skin-wave' value more rapidly. The phase angle, after reaching peak lag, turns sharply towards the asymptotic value. For larger values of $\beta$, however, the phase lag may recede to 180°. We mark this trend for $\lambda = 10$, $\beta = 0{\cdot}25$. This anomaly occurs due to the fact that the amplitude of magnetic drag reaches its asymptotic value much earlier than the phase, and its real component may change sign before reaching the critical frequency. Examination of Figures 1–6 suggests that $\omega_0^*$ gives an appropriate indication of the range of validity of the two solutions.

I thank Dr R. S. Nanda for his help in the preparation of the paper. I am grateful to Prof. B. R. Seth for constant encouragement.

REFERENCES

(1) Glauert, M. B. *J. Fluid Mech.* **12** (1962), 625.
(2) Lighthill, M. J. *Proc. Roy. Soc. London, Ser. A* **224** (1954), 1.
(3) Zhigulev, V. N. *Rev. Mod. Phys.* **32** (1960), 828.

https://doi.org/10.1017/S0305004100041463 Published online by Cambridge University Press